Analysis of Cardiac Cells Field Potentials using Wavelet Transform

S Jacquir, B Xu, T Bakir, J-M Bilbault, S Binczak

Laboratoire LE2I UMR CNRS 5158, Université de Bourgogne, Dijon, France

Abstract

Based on the experimental model, in this study, the heart rate variability (HRV) is investigated at a microscopically level in a cardiac cells culture by analyzing the field potential (FP) signals using a wavelet transform. Our results suggest that wavelet analysis provides useful information for the assessment of dynamic changes and patterns of FP train.

1. Introduction

Heart rate variability (HRV) is a reliable reflection of the many physiological factors modulating the normal rhythm of the heart [1]. It shows that the structure generating the signal is not only simply linear, but also involves nonlinear contributions. HRV corresponds to the variation over time of the period between consecutive heartbeats and is predominantly dependent on the extrinsic regulation of the heart rate (HR). In our precedent studies, an experimental model of FP propagation in physiological and arrythmia conditions has been established [2–8]. Based on this model, in this study, the HRV is investigated at a microscopically level in a cardiac cells culture by analyzing the field potential (FP) signals using a time-frequency method. A number of alternative time-frequency methods are now available for signal analysis. Among them, the wavelet transform has emerged over recent years as the most favored tool by researchers for analyzing problematic signals across a wide variety of areas in science, engineering and medicine [9]. It is especially valuable because of its ability to elucidate simultaneously local spectral and temporal information from a signal by employing a window of variable width [10]. The aim of this work is to characterize the electrical activity of cardiac cells by applying wavelet transform on experimental signals. In first, synchronous multifocal FP recorded using a non-invasive technology based on 60 substrate-integrated microelectrode arrays are denoised using a wavelet based method. Then choosing a pattern representing the FP signal in a normal rhythm of cardiac cell, an adapted wavelet function called mother wavelet has been synthesized. Using a wavelet transform and this mother wavelet, a time-frequency decomposition of the FP train has been realized in the case of the normal and abnormal rhythms leading to extract FPs from the signal and to obtain easily characterizing parameters, such as FP duration and positions. Our results suggest that wavelet analysis provides useful information for the assessment of dynamic changes and patterns of FP train. Finally, using this method, we show that during a normal rhythm (constant frequency between FP signal), fluctuations appear in the FP duration. These local spontaneous variations in the FP duration may be a safety process protecting against microscopically discontinuous conduction, and abnormality of this natural process could contribute to the genesis of some heart arrhythmias.

2. Materials and methods

2.1. Field potential data generation and acquisition

Neonatal ventricular myocytes were prepared from 1 to 4 days-old Wistar rats by trypsin-based enzymatic dispersion as described previously [11]. The cell suspension was preplated twice in the culture medium composed of Ham's $F10$ medium supplemented with fetal calf serum (FCS) and penicillin/streptomycin (100 U/ml) in order to increase cardiomyocyte proportion. Cardiomyocyte-rich cultures ($> 90\%$) were seeded at a final density of 10^5 cells per cm^2 in the cultured medium. Cultures were incubated in a humidified incubator (95% air, 5% CO_2 at 37° C) and were used after 4-5 days of growth, a step at which confluent and spontaneously beating cell monolayers were obtained. CM were grown on multielectrode arrays (MEA) allowing non-invasive synchronous multifocal field potential (FP) recordings. The MEA consists of 60 substrate-integrated microelectrode arrays (8×8 matrix, 30 μm electrode diameter, 200 μm inter-electrode distance). Data were acquired and analyzed with a customized platform programmed with Matlab (Mathworks) in order to provide two-dimensional electrophysiological maps derived from these multisite FP recordings.

2.2. Continuous wavelet transform (CWT) background

The continuous wavelet transform (CWT) is a time-frequency analysis method which allows arbitrarily high localization in time of high frequency signal features. The CWT does this by having a variable window width, which is related to the scale of observation. A large selection of localized waveforms can be employed as long as they satisfy predefined mathematical criteria (described below). The wavelet transform of a continuous time signal, $x(t)$, is defined as:

$$T(s,\tau) = \frac{1}{\sqrt{s}} \int_{-\infty}^{+\infty} x(t) \Psi^*_{s,\tau}(t) dt, \tag{1}$$

where $\Psi^*_{s,\tau}(t)$ is the complex conjugate of the analyzing wavelet function related to the mother wavelet $\Psi(t)$ as

$$\Psi^*_{s,\tau}(t) = \frac{1}{\sqrt{s}} \Psi \left(\frac{t-\tau}{s} \right) dt \tag{2}$$

The scale $s \in \mathbb{R}^{+,*}$ corresponds to the width of the wavelet function $\Psi_{s,\tau}(t)$ and $\tau \in \mathbb{R}$ is the shift of wavelet along the time axis. In order to be classified as a wavelet, a function must satisfy certain mathematical criteria. These are:
1. It must have finite energy:

$$E = \int_{-\infty}^{+\infty} |\Psi(t)|^2 dt < \infty \tag{3}$$

2. If $\widehat{\Psi}(f)$ is the Fourier transform of $\Psi(t)$, i.e.

$$\widehat{\Psi}(f) = \int_{-\infty}^{+\infty} \Psi(t) e^{-i2\pi ft} dt \tag{4}$$

then the following condition must hold:

$$C_g = \int_0^{+\infty} \frac{\left|\widehat{\Psi}(f)\right|^2}{f} df < \infty \tag{5}$$

This implies that the wavelet has no zero-frequency f component, i.e. $\widehat{\Psi}(0) = 0$, or to put it another way, it must have a zero mean. Equation 5 is known as the admissibility condition and C_g is called the admissibility constant. The value of C_g depends on the chosen wavelet.
3. For complex (or analytic) wavelets, the Fourier transform must both be real and vanish for negative frequencies. For its practical implementation the CWT is computed over a finely discretized time frequency grid. This discretization involves an approximation of the transform integral (i.e. a summation) computed on a discrete grid of scales s and position τ on the time axis. In general, the wavelet transform is approximated in this way over each time step for a range of wavelet scales. After given the conditions of admissibility and existence of the wavelet, we use a wavelet transform for denoising experimental FP signal, then an adapted wavelet mimicking the FP signal is synthesized to recognize a FP pattern in an experimental signal.

3. Results

3.1. Denoising field potential signal

A multilevel 1-D stationary wavelet decomposition using the Haar wavelet is applied to the experimental signal. This decomposition process produces two sets of coefficients: approximation coefficients and detail coefficients (see Fig. 1). These vectors are obtained by convolving the

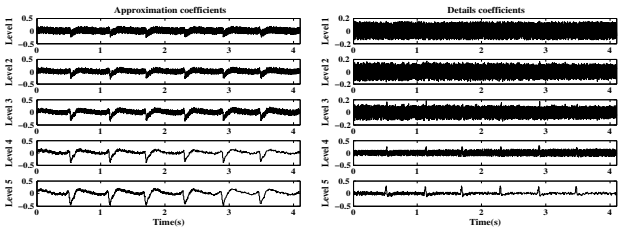

(a) (b)

Figure 1. Approximations (a) and details (b) coefficients resulting from the wavelet decomposition of a signal of FP train.

signal with the low-pass filter for approximation, and with the high-pass filter for detail. Then, after removing the detail coefficients corresponding to the levels $\{1,2,3\}$ and keeping the coefficients of approximation of all levels, a signal is reconstructed using the inverse discrete transform. The signal obtained in this manner is the denoised signal (see Fig. 2). Our experimental setup allows us to have 60

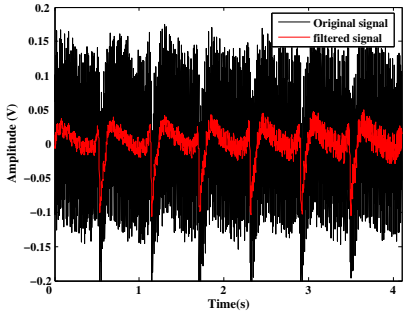

Figure 2. Original (black color) and denoised (red color) signal of field potentials.

signals simultaneously. These signals are distributed spatially and correspond to the configuration of the microelectrode array. Taking some signals as examples, the result of denoising is illustrated in the Fig. 3.

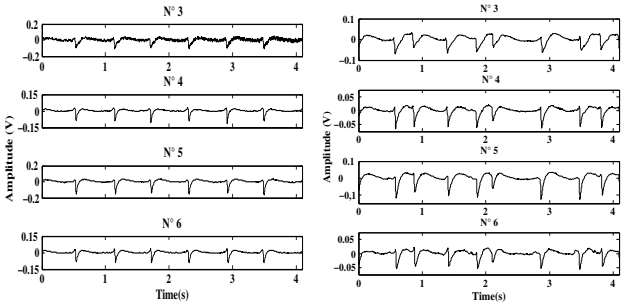

(a) (b)

Figure 3. Examples of denoised signals corresponding to electrodes $\{3,4,5,6\}$ after applying the wavelet decomposition. (a) (respectively (b)) shows a regular rhythm (respectively an arrhythmic signal).

3.2. Construction of adapted wavelet pattern of Field Potential

The wavelet coefficients in the CWT represent the degree of correlation between a wavelet mother function and the FP signal. Therefore, the choice of the wavelet basis is crucial for the accurate representation of the FP signal in the wavelet space. Using pattern defined from the FP experimental signal, an admissible wavelet for CWT is designed [12]. The principle for designing a new wavelet for CWT is to approximate a given pattern using least squares optimization under constraints leading to an admissible wavelet well suited for the pattern detection using the continuous wavelet transform [12]. This adapted wavelet named "field potential (FP) wavelet" has a norm equal to 1, so it respects the conditions ((3) and (4)). The pattern is approximated in the interval $[0,1]$ by least squares fitting using a projection on the space of functions orthogonal to constants. Depending on the experimental signal, the FP can be have different patterns, so some patterns of FP are illustrated in the Fig. 4.

4. Results

4.1. Field potential patterns recognition

Depending on experimental conditions and characteristic of cardiac cells, the FP signal to noise ratio (SNR) is very low. Then for investigating the activation map of FP generation and the map of the FP propagation, it is necessary to detect the presence of the FP in a signal. It is also

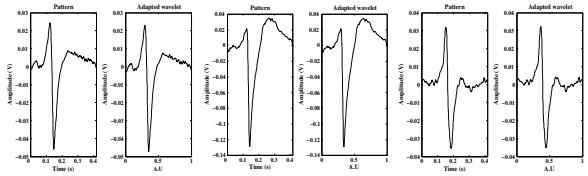

Figure 4. Different patterns constituting the experimental signal of field potentials train and adapted wavelets built from these patterns.

useful to classify the experimental signal between FP signal and artefactual signal. A good spatial localization and a good frequency localization of the FP can be performed using the CWT and the FP wavelet. So, using the CWT and the FP wavelet designed in the Fig. 4(a), the wavelet coefficients have been computed. These coefficients represent the degree of correlation between a wavelet mother function (FP wavelet) and the FP signal. The Fig. 5 illustrates the correlation image between the FP wavelet and the FP signal. The maximum of correlation is obtained for a specific scale s and a position τ. These correlation results give us also the number N of FP included in an experimental signal of FP train. The number N is the same for all electrodes in the case of the normal rhythm, it is variable and different on each electrode in the arrhythmic case.

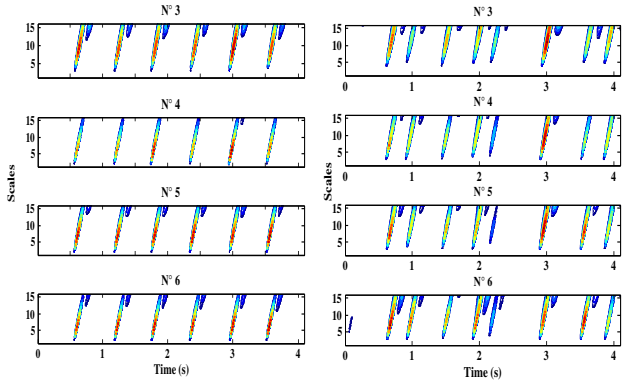

(a) (b)

Figure 5. Contour plots of the wavelet coefficients corresponding to electrodes $\{3,4,5,6\}$ given by the CWT using the FP wavelet.

4.2. Relationship between FP duration and FP frequency

Depending on N, for each FP, a local maximum is found in the wavelet coefficients corresponding to this FP. This local maximum illustrates the relationship between the scale s and the temporal position τ of the FP (see Fig. 6). Our hypothesis is that the scale s can be considered like as

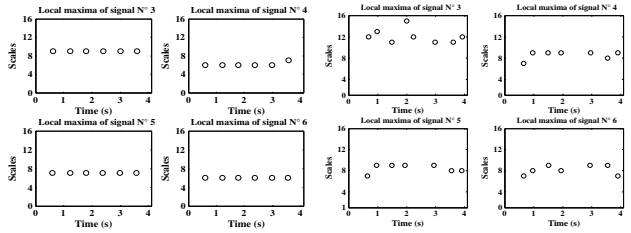

(a) (b)

Figure 6. Local maxima of FP pattern corresponding to electrodes $\{3,4,5,6\}$ in the normal rhythm (case (a)) and arrythmia signal (case (b)).

the FP duration and the temporal position τ can be used to determine the interspike interval (ISI) between successive spikes which represents the period of the FP pattern. The Fig. 6(a) illustrates that for a normal rhythm, small fluctuations appear in the FP duration but the ISI is constant. These local spontaneous variations in the FP duration may be a safety process protecting against microscopically discontinuous conduction (see Fig. 7(a)), and abnormality of this natural process could contribute to the genesis of some heart arrhythmias (see Figs. 6(b) and 7(b)). Considering also the approximation that the FP pattern represents the action potential derivative. We can approximate the action potential duration (APD) by the FP duration and the action potential (AP) frequency by the FP frequency. Seeing Fig. 7(a), there is a "stability relation" between the action potential duration (APD) and the frequency of action potential (AP). In the arrhythmic case, this stability can't be observed (see Fig. 7(b)), that means the variation of the APD and the frequency of AP simultaneously between successive spikes could be a factor initiating arrhythmia in the heart.

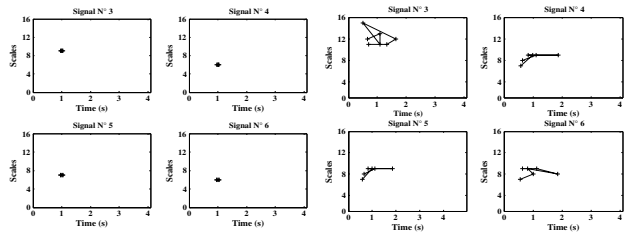

(a) (b)

Figure 7. Relationship between the FP duration (scale) and the FP period corresponding to electrodes $\{3,4,5,6\}$. Normal rhythm (case (a)) and arrythmia signal (case (b)).

5. Discussion and conclusions

In this work, HRV has been investigated in neonatal rat cultured CM. This study is based on the use of the wavelet transform (WT). According to the results presented here, the WT is an useful tool which can increase the SNR of the experimental data. It could be used to discriminate different signals. The WT property allows an analysis of HRV with accuracy. These investigations at cellular level may be helpful in the comprehension of the HRV.

References

[1] Acharya UR, Joseph KP, Kannathal N, Lim CM, Suri JS. Heart rate variability: a review. Med. Bio. Eng. Comput. 2006; 44:1031-1051.

[2] Jacquir S, Binczak S, Rosse M, Vandroux D, Laurent G, Athias P, Bilbault JM. Multisite Field Potential Recordings and Analysis of the Impulse Propagation Pattern in Cardiac Cells Culture. IEEE Computers in Cardiology Proceedings. 2007; 34: 125-128.

[3] Athias P, Jacquir S, Tissier C, Vandroux D, Binczak S, Bilbault JM, Rossé M. Excitation spread in cardiac myocyte cultures using paired microelectrode and microelectrode array recordings. Journal of Molecular and Cellular Cardiology, Elsevier. 2007; 42: S3.

[4] Jacquir S, Binczak S, Vandroux D, Laurent G, Athias P, Bilbault JM. Cardiac Arrhythmias Induced by an Electrical Stimulation at a Cellular Level. IEEE Computers in Cardiology Proceedings. 2008; 35: 625-628.

[5] Laurent G, Jacquir S, Binczak S, Vandroux D, Bouchot O, Wolf JE, Athias P, Bilbault JM. Establishing a novel in vitro model for the study of spiral waves during arrhythmia. European Heart Journal. 2008; 29(166).

[6] Jacquir S, Tissier C, Vandroux D, Binczak S, Bilbault JM, Rossé M, Athias P. Paired microelectrodes and microelectrode array analysis of cardiac impulse propagation in cardiomyocyte cultures. Fundamental Clinical Pharmacology. 2008; 22(1): 51-52.

[7] Jacquir S, Laurent G, Vandroux D, Binczak S, Bilbault JM, Athias P. In vitro simulation of spiral waves in cardiomyocyte networks using multi-electrode array technology. Archives of Cardiovascular Diseases, Elsevier. 2009; 102(1): S63.

[8] Athias P, Jacquir S, Laurent G, Vandroux D, Binczak S, Bilbault JM. In vitro simulation of spiral waves in cardiomyocyte networks using multi-electrode array technology. European Journal of Heart Failure Supplements. 2009; 8(963).

[9] Mallat S. A Wavelet Tour of Signal Processing. Academic Press. 2nd Edition. 1999.

[10] Addison PS. Wavelet transforms and the ECG:a review. Physiol. Meas. 2005; 26: R155-R199.

[11] Grynberg A. Primary rat cardiac cell culture: diet of the mother rats as a determinant parameter of cardiomyoblast production from neonates. Biol. Cell. 1986; 57: 89-92.

[12] Misiti M, Misiti Y, Oppenheim G, Poggi J-M. Wavelets and their applications. ISTE Ltd. 2007.

Address for correspondence:

Dr Sabir Jacquir

Laboratoire d'Electronique, Informatique et Image (LE2I UMR CNRS 5158), Université de Bourgogne, 9 avenue Alain Savary, BP 47870, 21078 Dijon, France,

sjacquir@u-bourgogne.fr